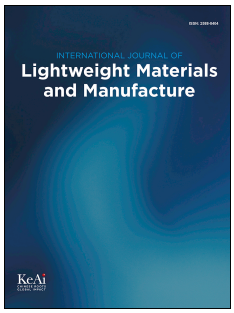

Manufacture and Characterization of Lightweight Sand-Plastic Composites Made of Plastic Waste and Sand: Effect of Sand Types

Salih MEKIDECHE, Mansour ROKBI, Zine El Abidine RAHMOUNI, Resego Phiri, Sanjay Mavinkere Rangappa, Suchart Siengchin

PII: S2588-8404(24)00081-7

DOI: https://doi.org/10.1016/j.ijlmm.2024.08.004

Reference: IJLMM 337

To appear in: *International Journal of Lightweight Materials and Manufacture*

Received Date: 1 April 2024

Revised Date: 22 July 2024

Accepted Date: 15 August 2024

Please cite this article as: S. MEKIDECHE, M. ROKBI, Z.E.A. RAHMOUNI, R. Phiri, S. Mavinkere Rangappa, S. Siengchin, Manufacture and Characterization of Lightweight Sand-Plastic Composites Made of Plastic Waste and Sand: Effect of Sand Types, *International Journal of Lightweight Materials and Manufacture*, https://doi.org/10.1016/j.ijlmm.2024.08.004.

Manufacture and Characterization of Lightweight Sand-Plastic Composites Made of Plastic Waste and Sand: Effect of Sand Types

Salih MEKIDECHE[1,2], Mansour ROKBI[1], Zine El Abidine RAHMOUNI[3], Resego Phiri[4], Sanjay Mavinkere Rangappa[4*], Suchart Siengchin[4]

[1]Department of Mechanical Engineering, Faculty of Technology, University of M'sila, M'sila, Algeria.

[2]Laboratoire de Matériaux et Mécanique des Structures (LMMS), University of M'sila, M'sila, Algeria.

[3]Department of Civil Engineering, Faculty of Technology, University of M'sila, M'sila, Algeria.

[4]Natural Composites Research Group Lab, Department of Materials and Production Engineering, The Sirindhorn International Thai-German School of Engineering (TGGS), King Mongkut's University of Technology North Bangkok (KMUTNB), Bangkok -10800, Thailand.

***Corresponding Author:** mcemrs@gmail.com; mavinkere.r.s@op.kmutnb.ac.th

Manufacture and Characterization of Lightweight Sand-Plastic Composites Made of Plastic Waste and Sand: Effect of Sand Types

Abstract

Over the past decade, many types of waste have been exploited as feedstocks in different industries. Recycled plastics are among the waste sought for several civil engineering applications. In this work, various plastic-bonded sand composites based on polypropylene waste and silica sand were produced to serve as building materials in many construction applications. Many tests and analysis were carried out in this investigation. First of all, two initial used compounds (waste PP and various silica sand) were analyzed by using ATR-FTIR, XRF, and grain size distribution. In the second time, the different plastic-bonded sand composites were analyzed by using ATR-FTIR to assess their composition. On the other hand, mechanical, and physical tests such as three-point flexural strength, compressive strength, water absorption, and optical observation were applied on different produced composite samples, then the results were examined and analyzed. The results showed that the developed composites exhibit commendable mechanical properties, especially flexural and compression resistance, and minimal water absorption. It is worth noting that the plastic-bonded sand containing Khobana sand showed the highest flexural and compressive strength at 11.56±0.36 and 26.19±0.27 MPa, respectively, along with the lowest water absorption rate of 0.46%. This study confirms its contribution to enhancing sustainability and promoting the principles of the circular economy.

Keywords: Plastic-bonded sand, Waste polypropylene, Mechanical properties, Recycling, Sustainable construction.

Introduction

In recent years, there has been a significant global increase in both the production and usage of plastic. This surge can be attributed to the vital role that plastics play in various aspects of our daily lives [1-3], including packaging, electronics, household goods, agriculture, transportation, medicine, piping, insulation and furniture manufacturing [4]. The production of plastic has increased remarkably over the past 15 years. Although numerous initiatives have been implemented to regulate plastics, reports indicate a continuous surge in plastic production. Starting from 2 million tons in 1950, it escalated to 367 million tons in 2020. Projections suggest that the cumulative global plastic production may soar to 2600 million tons/year by 2050 unless there's a global consensus to prohibit its proliferation [5]. The growing interest in plastic stems from its numerous advantages, such as being lightweight, waterproof, flexible, durable, and cost-effective. However, alongside these benefits come significant drawbacks, including poor mechanical properties, non-biodegradability, and susceptibility to temperature changes[6]. One of the most pressing issues associated with plastic use is the accumulation of plastic waste worldwide, which poses a severe environmental burden due to its resistance to natural degradation processes [7]. This waste contaminates soil and water, and obstructs stormwater drains and city drainage systems, leading to floods, property damage, and sometimes fatalities [8]. Additionally, it contributes to the proliferation of disease-carrying insects like mosquitoes [9, 10]. Consequently, scientists have been increasingly focused on finding solutions to the plastic waste problem for several years now. Investigations on plastic waste have thoroughly examined and extensively deliberated on a wide array of alternatives for its disposal [6, 11]. The most commonly utilized methods include mechanical recycling, incineration, and landfilling [11-13]. However, it is widely recognized that traditional landfilling and incineration can have adverse environmental effects [14]. Landfilling, for instance, can lead to long-term pollution of soil, groundwater, and nearby

surface water [4]. On the other hand, incineration may produce harmful byproducts such as toxic gases (e.g., carbon monoxide, furans, and polycyclic aromatic hydrocarbons), posing risks of localized toxicity to humans and the surrounding environment, and potentially disrupting the habitats of nearby animal species [15]. Moreover, the accumulation of ash containing significant quantities of microplastics at the bottom of incinerators poses a threat to ecosystems [6]. In contrast, mechanical recycling of plastic waste emerges as an environmentally friendly solution. Over the past decade, there has been a notable surge in research publications focusing on "plastic waste recycling," as evidenced by Figure 1.

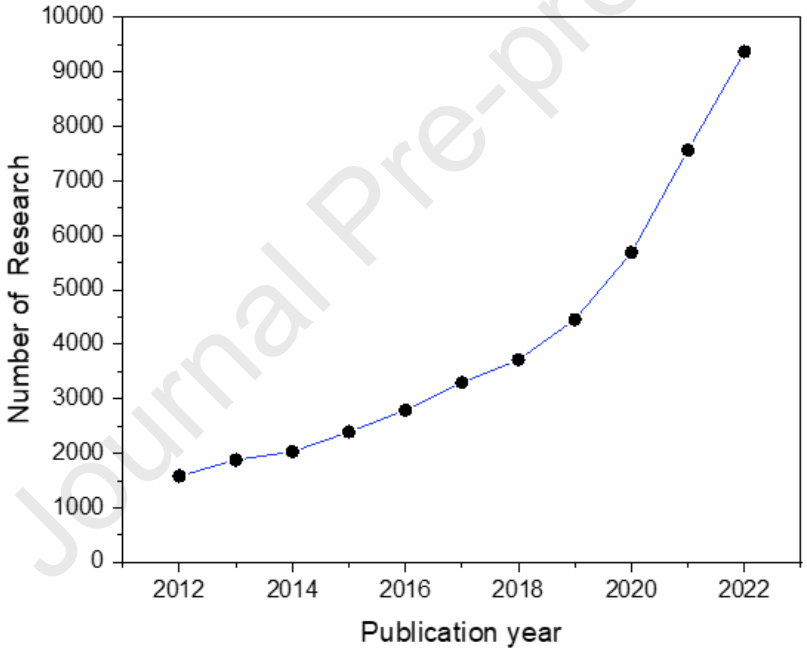

Fig. 1 Research papers on “plastic waste recycling” according to the Science Direct database.

The trend shown in Fig.1 can be attributed to the fact that mechanical recycling remains the most financially viable method for recycling plastic waste, with minimal environmental pollution concerns [1, 6, 7, 16]. However, the recovery rate of plastic waste remains relatively low, largely due to the low economic value of recycled plastics and a lack of technical support [17]. Globally, only around 20% of plastic waste is currently recycled [18]. Despite the relatively low rates of

plastic waste collection and recycling, recycled plastics still find utilization in diverse sectors such as construction, household items, fashion, electronics, plastic fabrics and more [19]. Utilizing plastic waste in civil engineering, particularly in building and construction projects, stands out as a significant avenue for its recovery and recycling [20]. Consequently, there's been a growing interest in this sector to develop more environmentally friendly materials. For instance, melt-blown LDPE water bags have been combined with sand to produce LDPE-bonded sand bricks with impressive compressive strength, reaching up to 27 MPa, indicating their strength and durability [8]. Similarly, Tulashie et al. [21] made significant efforts to convert unsorted plastic waste in Ghana into paving bricks. Their work demonstrated the feasibility of using plastic garbage to manufacture paving blocks, offering a potential solution to mitigate the rapid accumulation of plastic waste in the country. In a separate study, plastic sand bricks were effectively crafted from waste polyethylene and polypropylene [22]. These bricks exhibited promising outcomes, boasting a compressive strength of 12.43 MPa, minimal water absorption rates, and no fluorine content. Other efforts on sustainable construction materials involve combining low-density polyethylene residues with sand and coarse aggregates to construct paving blocks for road pavement. These blocks exhibited a compressive strength of 15.452 MPa, comparable to regular concrete paving blocks, along with improved water resistance [23]. Furthermore, research has explored the potential of waste plastic sand bricks as an eco-friendly alternative to traditional clay bricks, with results indicating enhanced compressive strength when adjusting the sand-to-plastic ratio [24, 25]. Additionally, some investigations have focused on creating composite materials, such as roof tiles, from recycled high-density polyethylene and sand dunes in varying proportions [26]. Optimal results were achieved with polymer roof tiles containing 30% sand dune and 70% high-density polyethylene.

However, the majority of studies in this area tend to focus more on incorporating plastic waste as aggregates [10, 27, 28] , as fiber [29] or as additives in concrete [30], while research on using plastic waste as a binder in concrete products remains relatively scarce. Presently, polypropylene (PP) is one of the most abundantly used plastic types, and it is generally more rigid and harder [31, 32]. In addition, PP is known to have also more chemical, heat, better elasticity, and toughness at normal temperature than some other thermoplastics such as polyethylene [33, 34]. That is why a large amount of waste PP can be recycled and can be also further used to replace virgin plastics in various engineering applications. Nowadays, many researches have been carried out to use a mixture of waste plastics (HDPE, LDPE, and PET) with sand to produce alternative construction materials such as pavement blocks [8, 10, 20, 35, 36], masonry bricks [37, 38]. However, only a few researchers have worked on a mixture of waste PP and sand to manufacture lightweight materials like plastic bricks [22]. Furthermore, many studies involving sand for material development lack a detailed exploration of the impact of different types of sand utilized. Therefore, this experimental investigation illustrated an attempt to develop a new low-cost and lightweight material consisting of silica sand as filler materials, and polypropylene waste as a binder. This lightened plastic-bonded sand composite can be used as alternative construction materials for pedestrian pavement, roof tiles, and decorative bricks. In the current paper, four different sand dunes are mixed with polypropylene waste to fabricate four various plastic-bonded sand composites. Three main goals were targeted through this work: firstly, the determining of the physical and chemical properties of two initial compounds used (waste PP and silica sands) by using ATR-FTIR, X-ray fluorescence, and grain size distribution. Secondly, explore the mechanical and physical properties of the obtained plastic-bonded sand composites based on flexural, compression, and water absorption tests. Thirdly, bring out the effect of sand types on the mechanical and physical performance of the resulting material.

Experimental

Raw materials

Waste polypropylene is one of the most solid wastes that takes a long time to biodegrade, so it makes sense to use this waste material in other industries to reduce its environmental impact [39]. This plastic waste was sourced from local recycling centers, where various types of plastic containers and items were collected. To facilitate sorting, these plastics were examined for indicative numerical codes commonly found on plastic packaging, which helped in identifying the type of plastic material. Once sorted, PP waste underwent a cutting process using a grinding machine aimed to reduce the plastic into smaller, uniform pieces, ranging in area from 5 mm^2 to 10 mm^2, as shown in Figure 2. Following the cutting process, thorough washing and drying of the chopped plastic pieces were carried out. This was essential to remove any contaminants or residues adhering to the plastic surfaces, thus ensuring the cleanliness and purity of the material. By meticulously washing and drying the plastic waste, any potential interference with subsequent analysis or experimentation was minimized, and the plastic material was rendered ready for detailed analysis and utility. One of the practical characteristics of polypropylene is its non-hygroscopic nature. This latter characteristic of PP, which goes up to 0.2%, can be a useful feature during molding. In other words, the moisture content does not affect the physical properties of PP during the molding process [40].

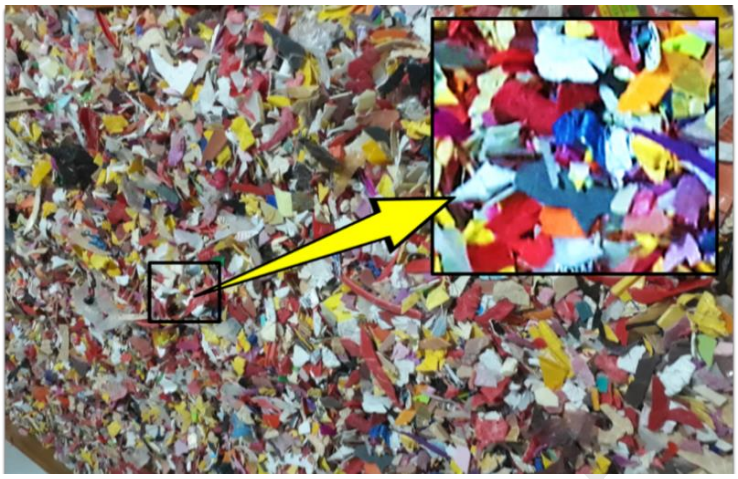

Fig. 2 Chopped polypropylene waste plastic pieces.

For this investigation, the silica sand used was readily available from local sources. Specifically, four distinct types of natural dune sand were gathered from various locations within the southern province of M'sila, Algeria, as indicated on the map displayed in Figure 3. To ensure the purity and suitability of the sand samples for experimentation, they underwent a cleaning process using water. This step aimed to eliminate any impurities or contaminants that might affect the properties of the sand. Once cleaned, the sand samples were left to dry thoroughly before being incorporated into the study.

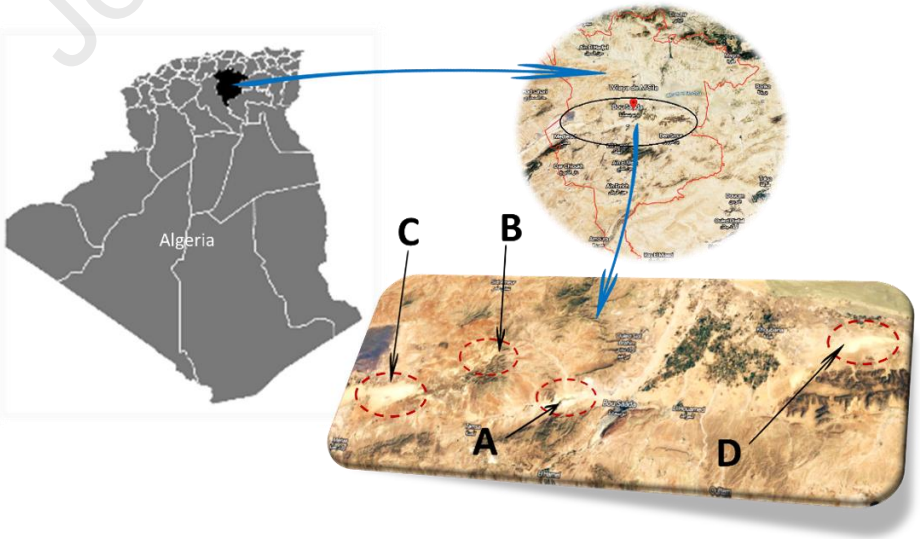

Fig. 3 M'sila Province map showing regions where sand dunes were collected; A) Oued Meitar; B) Ain Sbaa; C) Sidi Ameur; D) Khoubana

Materials analysis

ATR-FTIR analysis

The Attenuated Total Reflectance Fourier Transform Infrared (ATR-FTIR) technique offers an efficient means to swiftly determine various details concerning the chemical bonds and composition of different materials [41, 42]. In this study, the ATR-FTIR technique was adopted to investigate the chemical composition of four distinct types of silica sand using the Agilent Cary 630 FTIR spectrometer. After preparing the various types of sand, a suitable quantity (sample) of each type of sand was ground into a powder using a Mono-planetary grinder, the samples were then sieved to 80 µm size, and followed by analysis using ATR-FTIR. Different spectra were measured in the wavelength region from 4000 cm^{-1} to 400 cm^{-1} with an accuracy of 2 $cm^{-1.}$ Additionally, spectra for both virgin and waste polypropylene (PP) were obtained. This involved crushing both virgin and waste plastic materials, which were subsequently analyzed using the same apparatus. In other hand, the ATR-FTIR spectra of the new developed mixed plastic-bonded sand were recorded using the same techniques as previously mentioned above.

Chemical composition

The chemical composition of the four silica sands was analyzed using X-ray fluorescence (XRF) spectroscopy. XRF is a technique commonly used to determine the elemental composition of materials by measuring the fluorescent X-rays emitted when a sample is irradiated with X-rays [43]. In this study, silica sand samples were prepared for XRF analysis by being finely ground and homogenized to ensure representative sampling. The prepared samples were then placed into the Bruker S8 Tiger XRF instrument. As the X-rays interacted with the atoms in the sample, they

caused the emission of characteristic fluorescent X-rays. By detecting and analyzing these emitted X-rays, the elemental composition of the silica sand, including the concentrations of various elements present, could be determined.

Grain size analysis

To determine the grain size distribution curves of various silica sand samples, the analysis was conducted following the NF EN 933-1 standard. This method involves a systematic procedure utilizing vibrating sieves arranged in descending order by diameter [44]. In this analysis, the silica sand samples were thoroughly dried to remove any moisture content that could affect the results. Subsequently, a representative portion of the dried sample was weighed accurately. The next step involved the use of a series of vibrating sieves with progressively smaller mesh sizes. These sieves were arranged in a stack, with the sieve containing the largest openings placed at the top and the sieve with the smallest openings positioned at the bottom. Once the sieves were properly arranged, the prepared silica sand sample was placed onto the top sieve. The stack of sieves was then subjected to mechanical vibration, typically using a sieve shaker, to facilitate the separation of particles based on their size. After 15 minutes of shaking, the sieves were carefully removed from the stack, and the retained particles on each sieve were collected and weighed. The particle size distribution curves were then constructed based on the weights of particles retained on each sieve.

Fabrication

To manufacture plastic-bonded sand mixtures, a single-screw extruder machine was utilized to merge and melt the raw components. This machine is designed and manufactured by us. The specifications of the extruder machine are detailed in Table 1. Additionally, the extruder machine is externally heated by a three of electrical heating elements. To obtain the plastic-

bonded sand materials, firstly, the extruder was heated to a desired temperature (195 ± 5°C). After that, a mixture of sand and chopped waste plastics (PP) was fed into the screw through the hopper under the gravity action, as depicted in Figure 4. The rotation of the screw is ensured by a motor reducer. The resulting homogeneous paste (at 195 ± 5°C) was transferred to a mold, which was already heated to 200 ± 5°C, and then was compressed using a heat press to create plastic-bonded sand specimens of dimensions 4x4x16 cm3 as stated by [45]. After molding, the plastic-bonded sand products are allowed to cool and solidify, ensuring that they maintain their shape and structural integrity. Finally, the fabricated products may undergo finishing processes, such as trimming or sanding, to achieve desired surface textures or dimensions. Based on previous studies, different sample formulation was considered for the manufacturing of plastic-bonded sand. In the vast majority of work on plastic-bonded sand, the used ratios of plastic were taken between 20% and 50% [22, 23, 36, 45, 46]. The best results in flexural and compressive strength obtained of plastic-bonded sand composites were obtained for the

specimen formulation of 25 wt% of plastic [8, 36, 45]. To assess the impact of different types of sand on the mechanical and physical properties of the composites, four kinds of plastic-bonded sand samples were formulated according to Table 2.

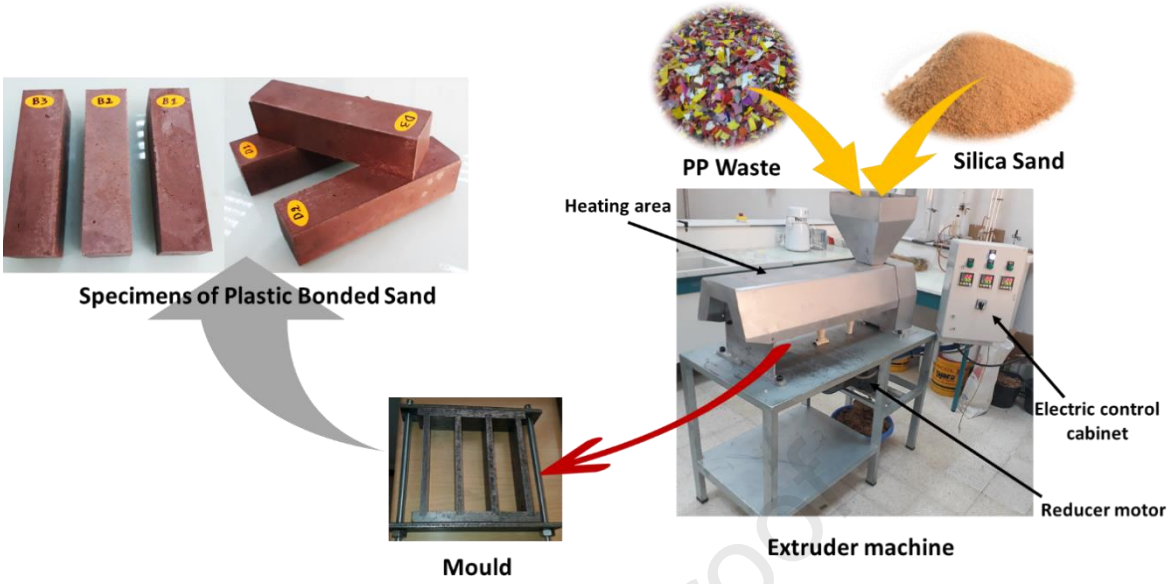

Fig. 4 Overview of the plastic-bonded sand fabrication methodology.

Table 1 Extruder characteristics

Parameters	**Values**
Screw root diameter	05 cm
Screw length	120 cm
Flight thickness	0.8 cm
Channel depth at end of screw	1.5 cm
Screw rotation speed	25 t/min
Max temp	400 °C

Table 2 Specimen formulation of plastic-bonded sand composites.

Sand source	**Designation of silica sand**	**PP waste by wt. %**	**Silica sand by wt. %**	**Designation of PBS***
Oued Meitar	Type A	25	75	Mat A

Ain Sbaa	Type B	25	75	Mat B
Sidi Ameur	Type C	25	75	Mat C
Khoubana	Type D	25	75	Mat D

*Plastic-bonded Sand

Water absorption test

To conduct a water absorption test for plastic-bonded sand material, the specimens were individually weighed using a precise scale to determine the initial weight. Subsequently, the specimens are fully submerged in water for 24 hours, to allow for complete saturation. After the immersion period, the specimens are removed from the water, gently blotted to remove excess moisture, and then weighed again to obtain their final weight. The water absorption percentage for each specimen is calculated using the difference between the final and initial weights, normalized to the initial weight, and expressed as a percentage. The formula for calculating the water absorption of a sample is given in Equation 1. This procedure allows researchers to evaluate the water absorption properties of materials, providing valuable insights into their performance and potential applications [47].

$$\text{Water absorption (\%)} = \frac{\text{Wet weight} - \text{Dry weight}}{\text{Dry weight}} \times 100 \qquad (1)$$

Mechanical tests

In this study, a three-point flexural strength test was conducted to assess the mechanical properties of various materials. The testing was performed using a YLE Universal TM/20 kN testing machine, operating at a crosshead speed of 0.4 mm/min, as depicted in Figure 5 (a), following ASTM D790-10 guidelines. Herein, the specimens were placed horizontally on two support points, with a load applied vertically at the midpoint until failure was reached. Throughout the test, measurements of applied load and corresponding deflection were recorded to calculate

flexural strength and modulus of elasticity. Each plastic-bonded sand formulation underwent testing on at least three samples to ensure the reliability and accuracy of the results.

Subsequently, the broken halves of the prisms resulting from the flexural test were subjected to a compressive test until failure. Load and deformation measurements were recorded throughout the test. This test was carried out utilizing the Hydraulic Pilot Pro Automatic Power and Control System with a capacity of 300 kN, applying a loading rate of 65 kN/min, as illustrated in Figure 5 (b). These testing procedures provide valuable insights into the mechanical behavior and structural integrity of plastic-bonded sand specimens, aiding in their suitability for engineering applications.

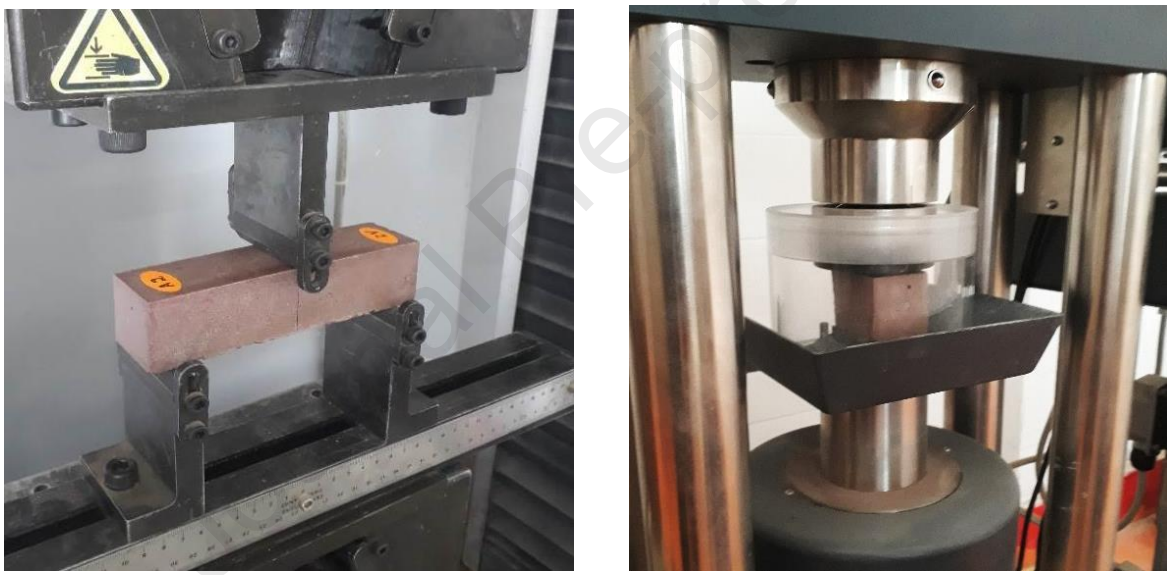

Fig. 5 Mechanical tests; a) Three-point flexural test; b) Compressive test

Optical analysis

In this study, an extensive optical analysis was conducted on the flexural fracture surfaces of different plastic-bonded sand samples. This analysis was performed using a sophisticated high-resolution optical microscope, specifically the Sunell IP CCD Camera, which allowed for detailed examination of the fracture surfaces at a microscopic level. The primary focus of this analysis was to evaluate the quality of the mixture comprising waste plastic and sand within the plastic-bonded

sand specimens. This involved assessing the level of homogeneity, distribution, and interaction of plastic and sand particles throughout the specimen. Additionally, the optical analysis aimed to identify any potential defects, inconsistencies, or irregularities within the material.

Results and discussions

Chemical composition of silica sand

The chemical analysis results (XRF) of different silica sand samples are summarized in Table 3. Notably, all analyzed sand samples exhibited a high silica (SiO_2) content, exceeding 93%. Specifically, Type C sand exhibited the highest silica content, reaching approximately 97%, followed by Type D at 95.64% sand and Type B sands with a silica content of around 95.61%. In contrast, Type A sand had the lowest silica content, around 93.6%. This variation in silica content among the different sand types underscores the significance of silica in determining the properties of the sand. Silica is a key component of sand and plays a crucial role in influencing its physical and mechanical properties. Understanding the silica content of sand samples is essential for selecting materials that meet specific performance requirements and ensuring the desired quality and performance of the final products. Higher silica content typically contributes to enhanced strength, stability, and durability of the sand material.

Table 3 XRF results for the composition of silica sands analyzed.

Composition of silica sand	Chemical composition of silica sand (%)					
	Current Study				Sand from El-Oued [42]	Sand from Biskra [48]
	Type A	Type B	Type C	Type D		
SiO_2	93.625	95.61	97.016	95.642	97.630	97.6

Al_2O_3	0.756	0.953	0.614	0.964	0.327	0.4
Fe_2O_3	0.696	1.009	0.888	1.007	0.042	0.5
CaO	2.349	0.659	0.467	0.657	0.564	1
MgO	0.058	0.107	0.010	0.110	0.613	<0.05
SO_3	0.073	0.096	0.076	0.095	0.037	-
K2O	0.300	0.394	0.268	0.394	0.067	<0.05
Na2O	0.000	0.000	0.000	0.003	0.542	0.06
P_2O_5	0.018	0.021	0.018	0.021	0.013	<0.05
TiO_2	0.094	0.098	0.065	0.099	0.005	<0.05
Cr_2O_3	0.059	0.088	0.095	0.088	-	-
Mn_2O_3	0.011	0.011	0.011	0.012	0.002	<0.05
ZnO	0.000	0.000	0.000	0.000	-	-
SrO	0.009	0.007	0.008	0.007	-	-

ATR- FTIR spectroscopy

The ATR- FTIR analysis provided valuable insights into the main compounds present in various silica sand samples. The infrared transmittance spectra of the collected samples are depicted in Figure 6. Table 4 provides a summary of the study of the infrared absorption spectrometry graphs. Typically, all the sand samples comprise primarily Quartz, Calcite, and Dolomite [49, 50]. Quartz constituted the predominant component in all types of silica sand, as evidenced by its high transmittance percentages. This dominance of Quartz is indicated by prominent peaks observed at 520 cm^{-1}, 710 cm^{-1}, 766 cm^{-1}, and 1007 cm^{-1} in the spectra [42, 50-53]. Interestingly, these peaks were most pronounced in type C sand, followed by type D sand, type B, and finally type A sand, aligning with the chemical composition determined through XRF analysis. Additionally, the

presence of Calcite is revealed by peaks at 872 cm^{-1} and 1420 cm^{-1} in the spectra [42, 52]. While type A sand exhibited prominent Calcite peaks, the remaining samples displayed smaller peaks.

The presence of dolomite in sand can significantly influence its properties and suitability for various applications. Dolomite, a mineral composed of calcium magnesium carbonate, enhances sand's physical and mechanical properties, including its strength, stability, and resistance to weathering. However, it's notable that certain sand samples, particularly those from the Algerian Sahara region, exhibit a lower presence or absence of dolomite. This variation in dolomite content can be attributed to geological factors and the specific origins of sand deposits in each region [54]. Geological processes and the depositional environment play crucial roles in determining the mineral composition of sands. In some regions, geological conditions may favor the deposition of sands with minimal dolomite content, while in others, dolomite-rich sands may be more prevalent.

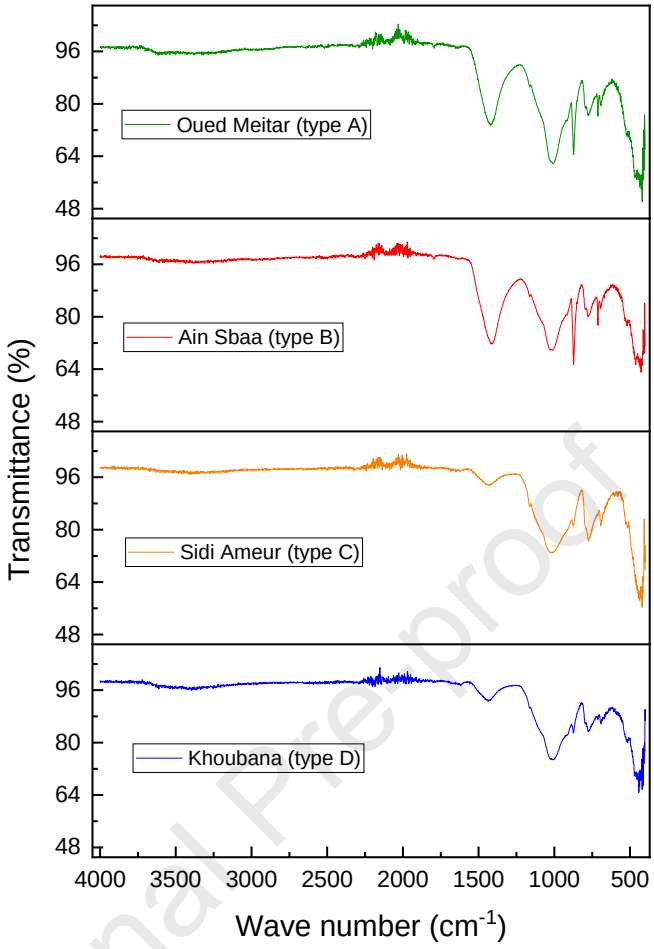

Fig. 6 FTIR spectra of different Sands.

Table 4 Main bands of IR absorption and associated functional groups.

Bond (cm^{-1})	Bond (vibration mode)	Compound	Ref
520	Si-O-Al	Quartz	[51]
710	Si-O-Si	Quartz	[42, 51]
766	Si-O	Quartz	[42, 50-52]
872	$(CO_3)^{-2}$	Calcite	[42, 52]
1007	Si-O-Si	Quartz	[50, 52]
1420	$(CO_3)^{-2}$	Calcite	[42]

The ATR- FTIR analysis was conducted on both virgin and waste polypropylene samples for comparison purposes. The infrared spectra of the two PP samples, revealing multiple distinct peaks are shown in Figure 7. Notably, at a wavenumber of 995 cm^{-1}, a functional group C–H was observed due to asymmetric vibrations of CH_3 [55]. Additionally, the peak at 1170 cm^{-1} was attributed to the asymmetric stretching vibrations of C-C [55-57], while the peak at 1373 cm^{-1} resulted from the symmetric deformation vibrations of CH_3 [55, 58]. Moreover, the band at 1468 cm^{-1} was associated with the asymmetric deformation of CH_3 or CH_2 vibrations [55, 57]. Furthermore, the band at 1730 cm^{-1} was assigned to combined vibrations and expansion of CO [55, 59]. The absorption spectrum at 2915 cm^{-1} represented the vibration of the CH_2 group in the primary polypropylene chain [55, 58]. Observing the two spectra in the figure did not reflect much variation between the distinctive bands [60]. Table 5 offers a comprehensive overview of the infrared spectra analysis, summarizing the observed peaks and their assignments.

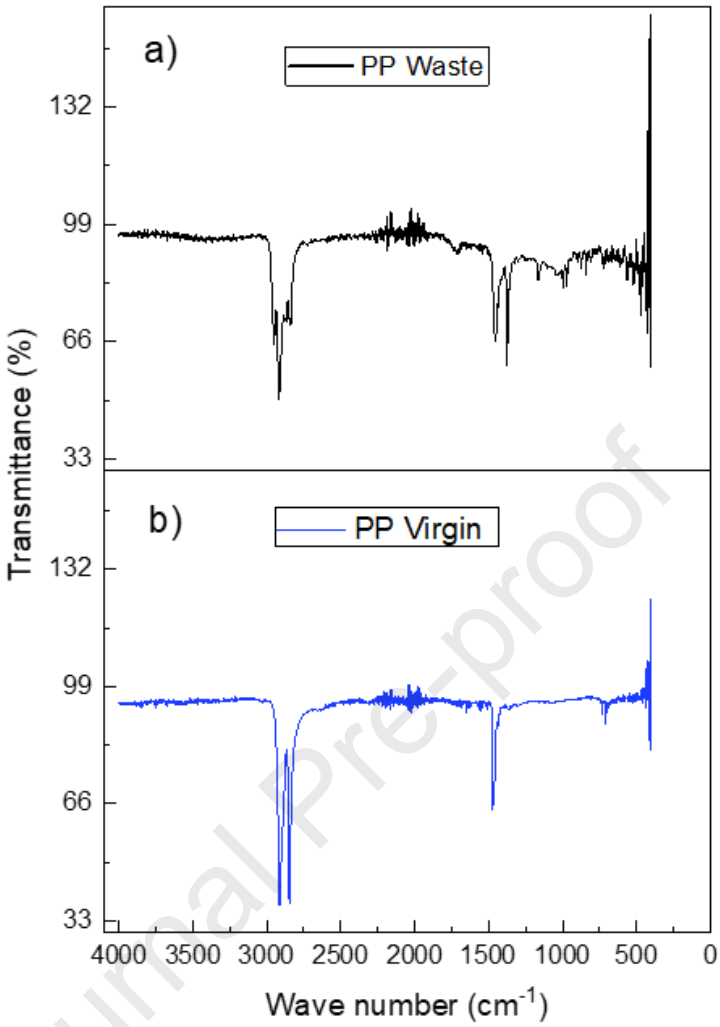

Fig. 7 ATR- FTIR spectra of PP a) PP Waste, b) PP Virgin.

Table 5 The main bands of FTIR absorption and associated bond vibration of PP

Bond (cm^{-1})	Bond (vibration mode)	Compound	Ref
995	CH_3	Alkyl groups	[55]
1170	C–C	Carbonyl compound—possibly ester or ketone	[55-57]
1373	CH_3	Alkyl groups	[55, 58]
1468	CH_3	Alkyl groups	[55, 57]

1730	C O	presence of carbonyl (C O) groups in ketones	[55, 59]
2915	CH_2	group vibration in the main PP polymer chain	[55, 58]

Generally, ATR-FTIR analysis is performed on the initial compounds used and the formed product. As was the case for ATR-FTIR of PP and different types of sand, the functional groups of various plastic-bonded sand samples were investigated by analyzing the spectra obtained. Figure 8 presents the ATR- FTIR spectra of the plastic-bonded sand composites. As can be seen in this figure, the spectra appear to have the same pattern for all the samples with minor differences. The slight change can be attributed to the physical interaction between the two ingredients [61]. For all spectra, the absorption at 1367 cm^{-1} 1460 cm^{-1} 2840 cm^{-1} 2910 cm^{-1} represent vibrations of CH_2, CH_3, and C-H bands, where it stands out the specific characteristics absorption of the PP matrix [62]. The characteristic absorptions appear at the wavenumbers 686 cm^{-1}, 780 cm^{-1}, 1050 cm^{-1} which are attributed to Si-O and Si-O-Si [21].

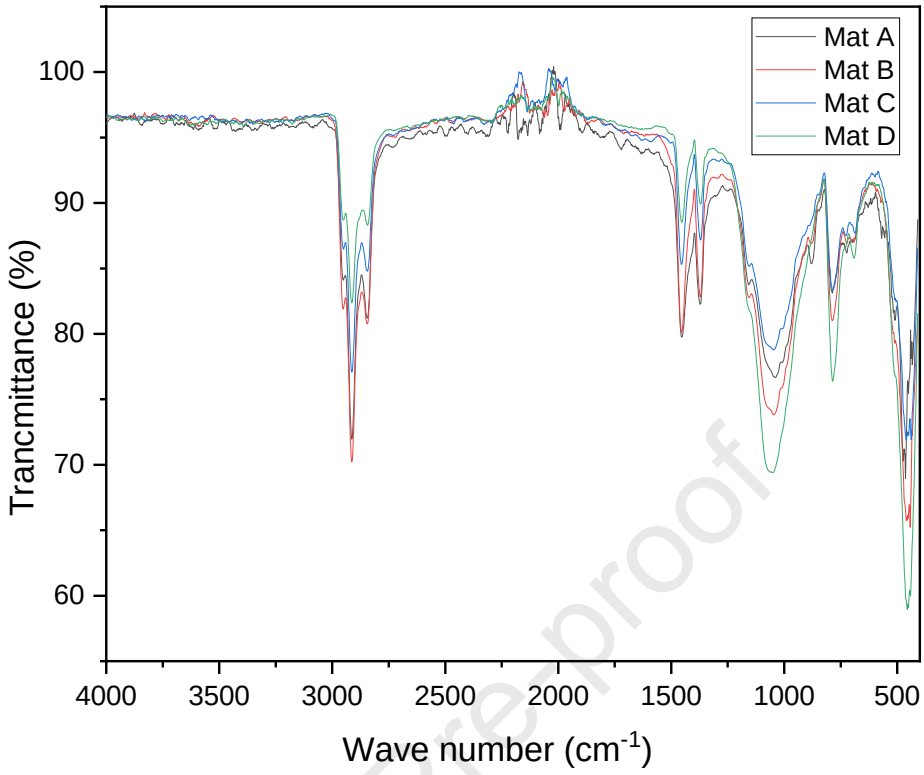

Fig. 8 ATR- FTIR spectra of Plastic-bonded sand composites.

Figure 9 presents the ATR- FTIR spectra of waste PP, sand type "D" and that of their composite. From this figure; all bands of two compounds (waste PP and sand) are visible after extrusion processing. It can be also reported that the ATR-FTIR spectra of the composite confirm the presence of Si-O and Si-O-Si within the PP matrix material. Furthermore, one of the most noticeable variations in the PP and its composites' spectra is the outstanding decrease in waste PP intensities bands [63]. According to Vilímová et al. [63] , this reduction is mainly due to the thermal treatment of PP plastic, but no structural changes are visible. In other work, Roberto López-Ramirez et al. have used FTIR analysis when studying the PP/ceramic waste composite properties. As a result, similar chemical structures of the composites are observed and no major

changes were signaled among the composites, this can confirm the type of interfacial contact mechanism via mechanical adhesion. The same observation was reported by [64].

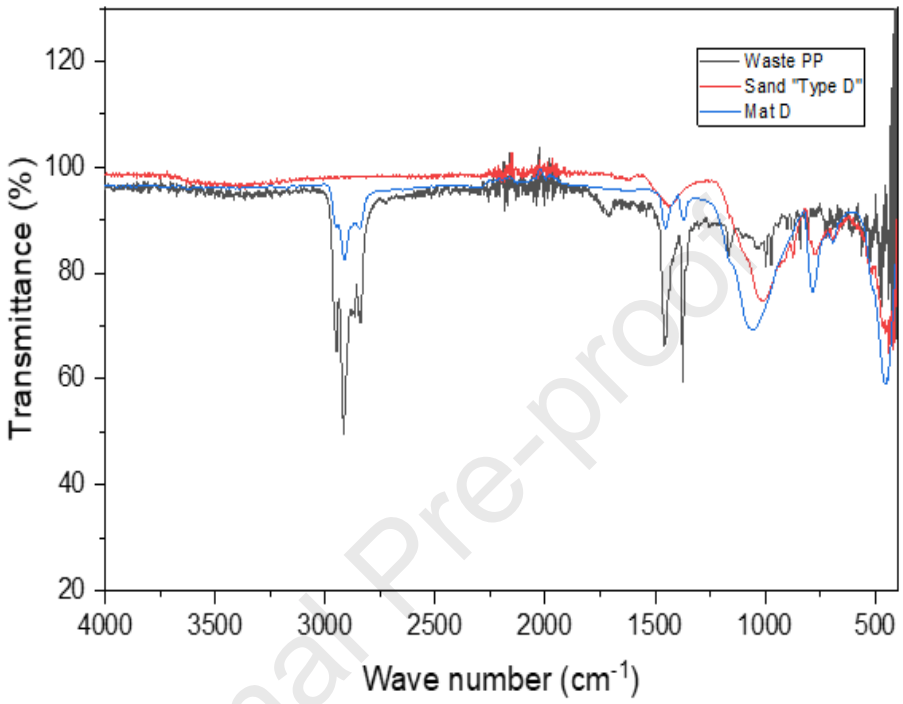

Fig. 9 ATR- FTIR spectra of PP Waste, Sand "Type D "and Mat D.

Grain size analysis

The grain size analysis of different types of sand involves determining the distribution of particle sizes within each sample. This analysis provides crucial information about the texture and characteristics of the sand, which can influence its suitability for various construction applications. In the study, the sand samples collected from different sand dunes naturally exhibited a mixture of particle sizes, which is typical in sedimentary environments. This variability in particle sizes

reflects the diverse geological processes that contribute to the formation of sand deposits. The sand grains were categorized based on their diameters into three main groups: coarse sand, medium sand, and fine sand. Coarse sand consists of larger particles with diameters ranging from 0.6 to 2 mm. These grains are visibly larger and can be felt easily between fingers. Medium sand, on the other hand, comprises particles with diameters between 0.2 and 0.6 mm. These grains are smaller than coarse sand but still perceptible to the naked eye. Fine sand is characterized by even smaller particles, with diameters ranging from 0.06 to 0.2 mm. These grains are much finer in texture and may feel almost like powder when handled.

Table 6 Quantitative analysis of the grain size diameter ranges for different sands.

Type of sand	Grain diameter ranges of sand (wt%)		
	Fine (0.06 – 0.2 mm)	Medium (0.2 – 0.6 mm)	Coarse (0.6 – 2 mm)
Type A	38%	58%	04%
Type B	61%	39%	-
Type C	47%	53%	-
Type D	60%	40%	-

Figure 10 visually represents the distribution of grain sizes within each category, helping to illustrate the variation in particle sizes present in the different types of sand dunes. This information is crucial for understanding the texture, porosity, permeability, and other properties of the sand, which are essential considerations for blending with waste propylene for composite fabrications. Furthermore, Table 6 provides a quantitative result of the grain size diameter ranges calculated from the particle distribution curve. The distribution of sand types D and B consists of up to 60 wt% of fine sand grains and approximately 40 wt% of medium sand grain size.

Conversely, sand type C comprises 47 wt% of fine sand grains and 53 wt% of medium sand grain size. Sand type A contains 38 wt% of fine sand grains, along with 58 wt% of medium sand grain size and 4 wt% of coarse sand grain size.

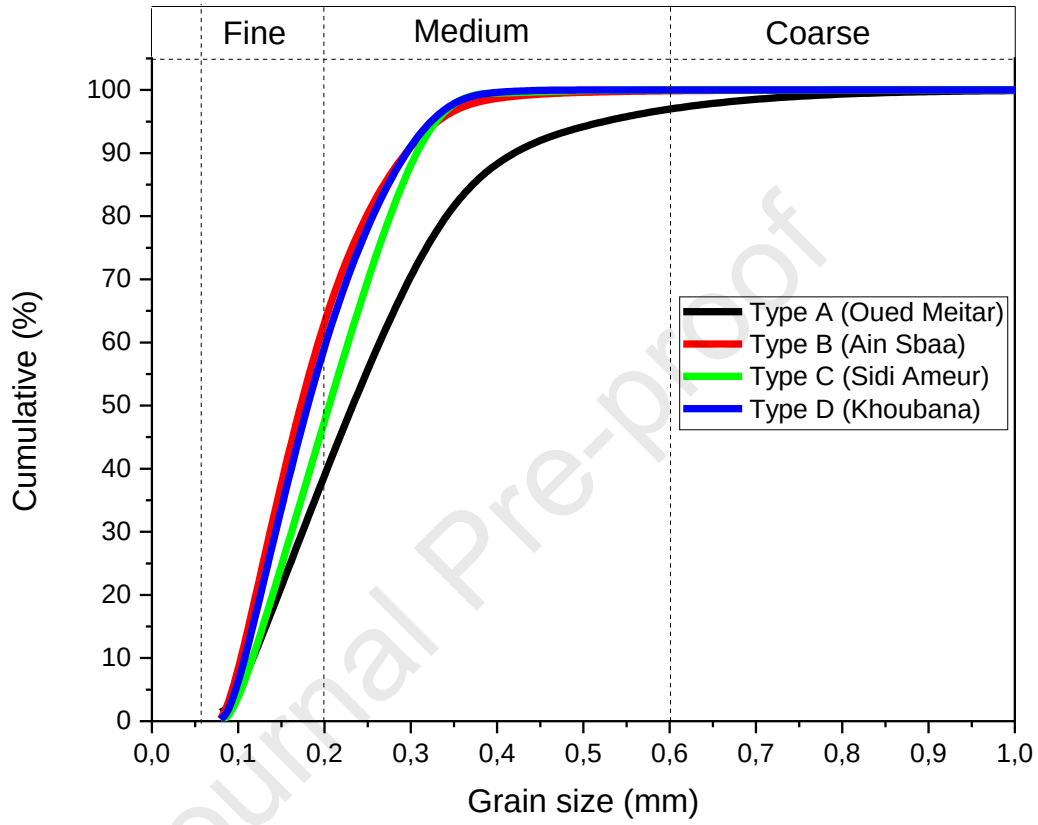

Fig. 10 Grain size distribution curve for different sands.

Water absorption

The water absorption test serves to assess the suitability of plastic-bonded sand for various environmental conditions, including wet, dry, or moist settings. Several factors influence the material's ability to absorb water, including the presence of pores within the material, the size of the sand particles, and the connectivity between these pores [38, 47, 65]. Additionally, the type of plastic used can impact water absorption, with research indicating that materials such as HDPE/sand exhibit lower water absorption percentages compared to other plastic waste mixtures like LDPE/sand and PETE/sand [38]. In this study, Table 7 displays the average water absorption

percentages, ranging from 0.46% to 1.42%. This variance may stem from differences in porosity ratios among the various plastic-bonded sand compositions and/or variations in the distribution of sand particle sizes. Research indicates that HDPE/fine sand mixtures tend to have fewer pores due to smaller grain particle sizes, resulting in a more densely packed mixture. Conversely, an abundance of internal pores in plastic-bonded sand can increase connectivity between pores [66].

Table 7 Water absorption of plastic-bonded sand specimens.

Material	Water absorption	Source
Mat A	1.43±0.07	Present work
Mat B	0.67±0.04	
Mat C	1.16±0.04	
Mat D	0.46±0.03	
HDPE/Sand	0.0634	[47]
PET /Sand	less than 1	[46]
LDPE/Sand	1.19	[14]

Therefore, the lower water absorption observed in "Mat B" and "Mat D" could be attributed to their well-distributed particle sizes, which reduces the presence of pores and minimizes interconnectivity between them.

Flexural strength

The three-point flexural strength of various plastic-bonded sand specimens was assessed by recording load-displacement curves using the Universal TM/20 kN testing machine. The results revealed a predominantly linear behavior in the tested specimens, as illustrated in Figure 11. Analysis of the curves indicated that Mat D exhibited the highest load capacity, reaching approximately 4200 N, accompanied by a maximum deflection of 0.54 mm at failure. Following

this, Mat B displayed a load capacity of 3000 N with a deflection of 0.45 mm, while Mat C demonstrated a load capacity of 2500 N and a deflection of 0.44 mm. Conversely, Mat A exhibited the lowest maximum load capacity, registering at 1900 N, along with a minimum displacement of 0.37 mm.

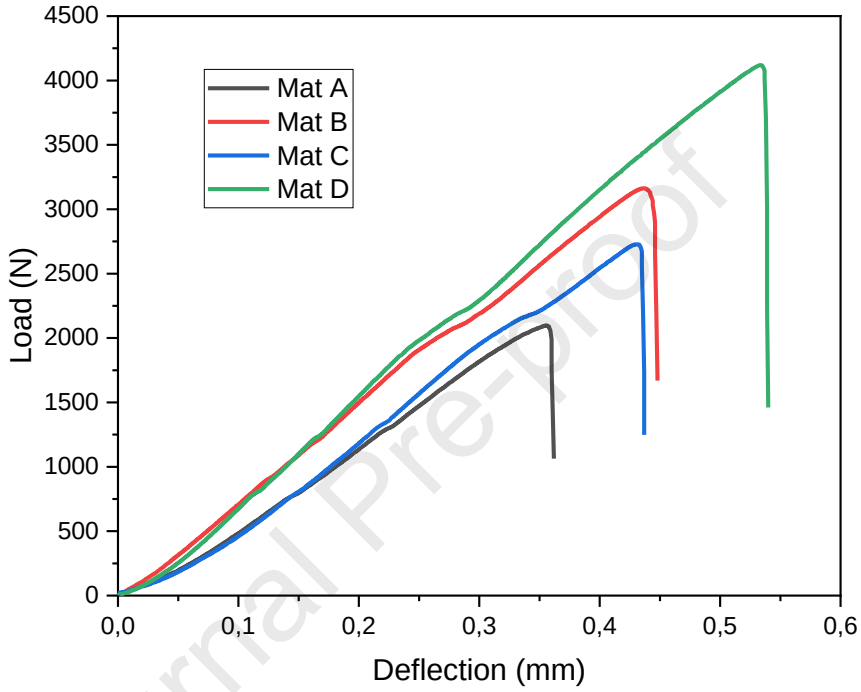

Fig. 11 Flexural test curves showing the load-displacement curves of the bonded materials**.**

Additionally, the flexural stress, flexural modulus, and flexural strain of the various tested plastic-bonded sand materials are depicted in Figure 12, with summarized results presented in Table 8. The findings underscore the significant influence of sand type on the flexural properties of the manufactured materials. Specifically, the determined flexural stresses were 5.45 MPa for Mat A, 9.08 MPa for Mat B, 7.26 MPa for Mat C, and 11.56 MPa for Mat D. The notable performance of Mat D and Mat B in three-point flexural strength can be attributed to their relatively uniform grain size distribution, lower porosity degree and reduced interconnectivity between pores [38, 47, 66].

A similar trend was evident in the flexural modulus results, with higher values observed for Mat D (1557 MPa) and Mat B (1450 MPa) composites. These elevated flexural modulus values may indicate a more effective interfacial transition zone [65]. Conversely, materials Mat A and Mat C exhibited the lowest flexural modulus values, measuring 1061.52 MPa and 1137.44 MPa, respectively. Furthermore, the average flexural strain values for all tested plastic-bonded sand specimens followed a consistent trend, with Mat D, Mat B, Mat C, and Mat A displaying flexural strain ranges of 0.70%, 0.66%, 0.61% and 0.58%, respectively. These results provide valuable insights into the structural performance of each material, highlighting variations in flexural properties based on sand type and composition. Table 8 summarizes the mean values found for the different plastic-bonded sand configurations. These values are compared with others sand-plastic composites recently proposed in literature. As indicated by Table 8, the flexural stresses of the studied plastic-bonded sand composites are distinctly found much higher than those formulated with LDPE/Sand [47], HDPE/Sand [47], and PET/Sand [46]. This distinction appears to be mainly attributed to the nature of used waste plastics. Dalhat and Wahhab [67] investigated bounded cemented structures to assess the potential use of recycled plastics (HDPE and PP). According to a prior study [67], recycled PP exhibited bending strengths that were three times greater than those of ordinary cement concrete and five times more than those of asphalt concrete. On the other hand, the authors deduced that recycled PP is more efficient than recycled HDPE in such applications.

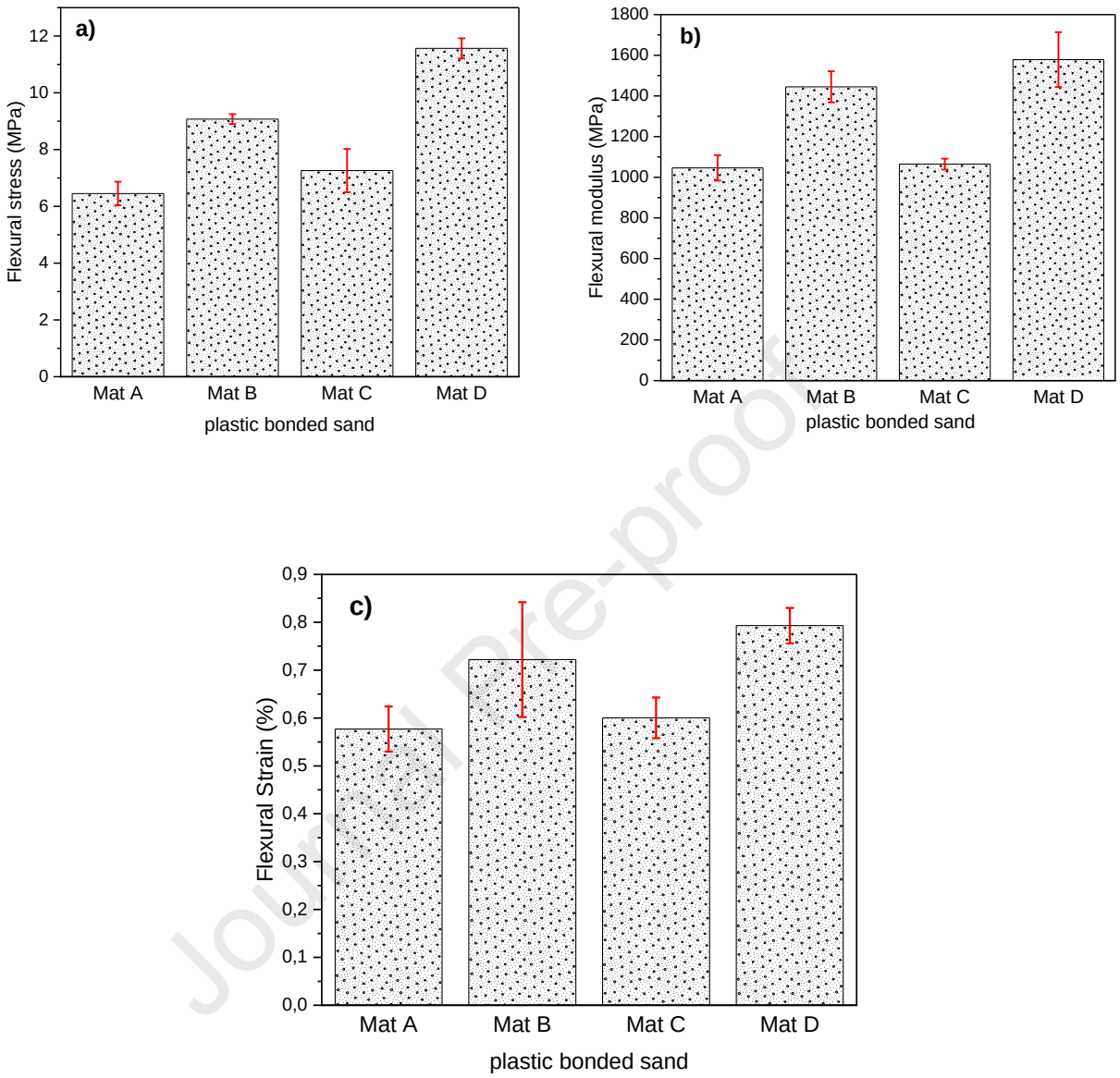

Fig. 12 Flexural properties of different plastic-bonded sand materials a) flexural stress, b) flexural modulus, and c) flexural strain.

Table 8 Flexural test results of tested plastic-bonded sand specimens

Designation		Specimens	Stress (MPa)	Mean Stress (MPa)	Strain (%)	Mean Strain (%)	Modulus of flexion (MPa)	Mean Modulus of flexion (MPa)	Ref
Plastic-bonded sand	**Mat A**	**1**	6.04	6.48	0.53	0.58	983.64	1061.52	**Present work**
		2	6.55		0.62		1092.45		
		3	6.87		0.58		1108.46		
	Mat B	**1**	9.25	9.1	0.74	0.66	1368.33	1450.24	
		2	9.16		0.65		1521.44		
		3	8.9		0.6		1460.96		
	Mat C	**1**	7.41	7.31	0.64	0.61	1037.87	1137.44	
		2	8.02		0.64		1091.54		
		3	6.5		0.56		1282.91		
	Mat D	**1**	11.9	11.63	0.79	0.7	1713.33	1557.94	
		2	11.8		0.83		1443.54		
		3	11.21		0.76		1516.96		
LDPE/Sand				5.13					[47]
HDPE/Sand				6.24					
PET/Sand				2.55					[46]

Compressive strength

The compression results of the plastic-sand bricks revealed significant variations in compressive strength across different compositions. Fig. 13 depicts the relative compressive strength. Among the tested materials, the plastic-bonded sand containing Khoubana sand, designated as MAT D, exhibited the highest compressive strength of 26.19 MPa indicating their suitability for applications requiring robust structural support. This was followed by MAT B with a compressive strength of 22.07 MPa . Conversely, the lowest compressive strength was observed in the plastic-bonded sand incorporating Oued Meitar sand, denoted as MAT A, which recorded a compressive strength of 17.92 MPa. This trend of lower compressive values in MAT A and MAT C is attributed to the presence of larger sand particle sizes within their structures [8]. Additionally, porosity and interconnectivity between pores are other defects that may affect the compressive strength of sand plastic composites. Research by Baris and Tanacan [68] highlighted that a higher degree of pore interconnectivity leads to larger pore size dispersion and decreased strength. Overall, the compression results reveal valuable insights into the material structural integrity and load-bearing capabilities.

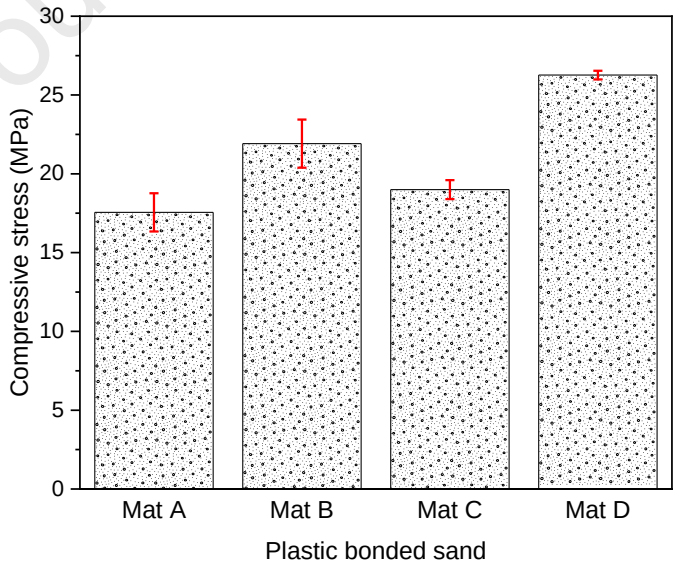

Fig. 13 Compressive behavior of tested plastic-bonded sand materials.

Table 9 resumes the critical load and stress values registered during the compressive test of diverse sand-plastic composites. Once again, the manufactured composites record the highest values compared to LDPE/sand [20], PET/Sand [46], PE/River sand [24], and HDPE/fine aggregates [38].

Table 9 Compressive test results of the plastic-bonded sand specimens

Designation		Specimens	Load (kN)	Mean Load (kN)	Stress (MPa)	Mean Stress (MPa)	Ref
Plastic-bonded sand	Mat A	1	29.54	28.57	18.64	17.92	Present work
		2	26.14		16.34		
		3	30.03		18.77		
	Mat B	1	35.81	35.6	22.38	22.07	
		2	37.5		23.44		
		3	33.49		20.39		
	Mat C	1	31.24	30.96	19.53	19.17	
		2	31.36		19.6		
		3	30.29		18.39		
	Mat D	1	41.64	41.85	26.03	26.19	
		2	42.33		26.54		
		3	41.58		25.99		
LDPE/Sand						16.66	[20]
PET/Sand						11.50	[46]

PE/River sand	12.28	[24]
HDPE/fine aggregates	08.37	[38]

Optical Microscopy

In concrete technology, the petrographic and nondestructive analytical methods can be used to analyze the uniformity of structure. These methods show if the materials exhibit uniform distribution in their microstructures and if their structural integrity is adequate [69]. The microscopic examination of the flexural fracture surfaces of the specimens, depicted in Figure 14, reveals crucial insights into their structural integrity. Overall, all prepared materials exhibit a commendable level of homogeneity. However, upon closer inspection of Mat A and Mat C in Figures 14 (a)-(c), several defects become apparent, including pores, interconnectivity issues, and poor interfacial transition zones. The inadequate interfacial transition zone can be attributed to the failure of plastic waste to effectively fuse with sand particles, leading to air entrapment in this region [65]. Consequently, these defects contribute to lower compression and flexural strength, as well as increased water absorption rates.

Conversely, as depicted in Figures 14 (b)-(d), the sand particles within the structure are thoroughly encapsulated and mechanically bound by the plastic binder showing good structural integrity. Additionally, a reduction in porosity and the presence of finer sand particles are observed. These characteristics contribute to a composite with enhanced strength and improved water absorption properties.

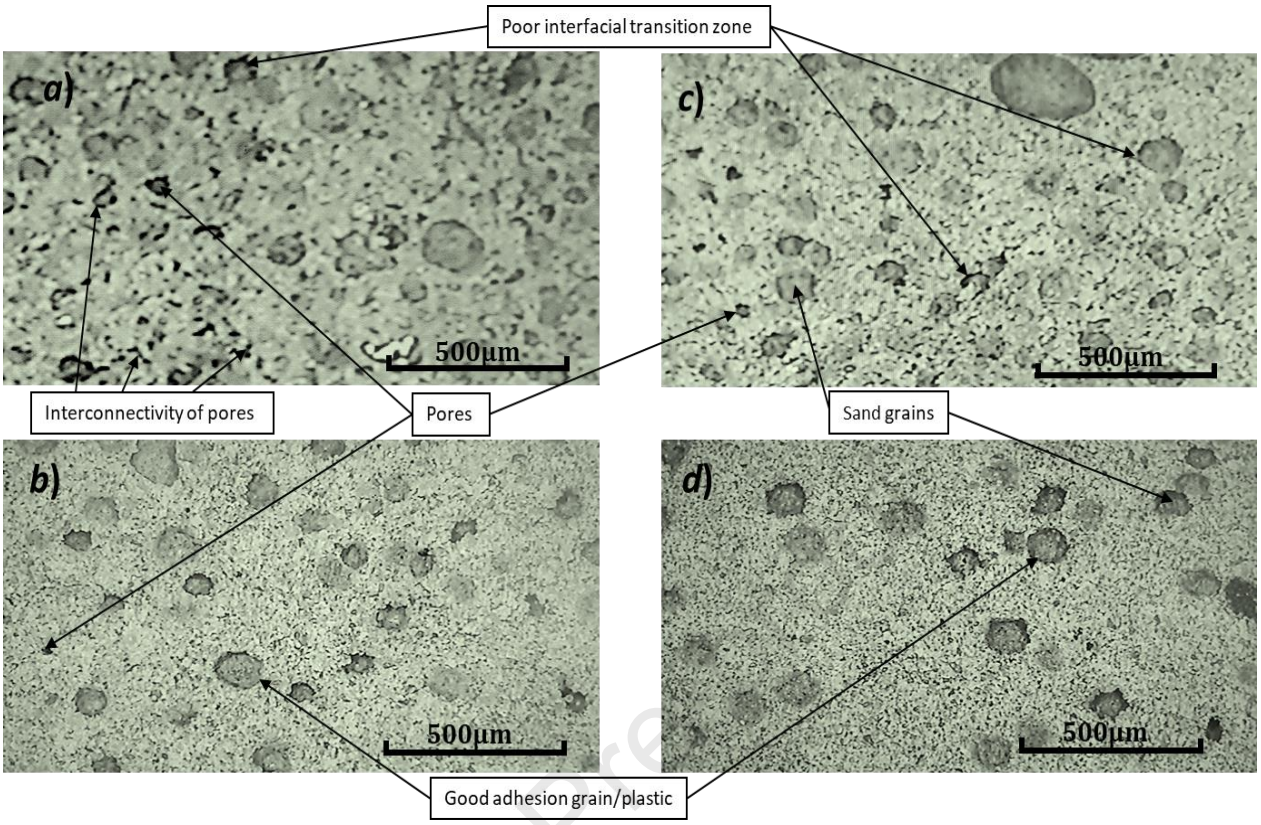

Fig. 14 Optical Microscopic picture of fracture surfaces of specimens of flexural test of plastic bonded sand, a) Mat A, b) Mat B, c) Mat C, d) Mat D.

Conclusions

This study focused on the development and characterization of plastic-bonded sand composites for potential applications in civil engineering. Through a comprehensive series of tests and analysis, several key findings have emerged. Firstly, the utilization of waste polypropylene as a binder, along with different types of silica sand as fillers, has shown promise in creating sustainable construction materials.

The mechanical properties, including flexural and compressive strength, were evaluated, with notable variations observed based on the type of sand used. The composite fabricated with

Khoubana sand (Mat D) exhibited superior mechanical properties compared to the other materials. Following this, the Ain Sbaa (Mat B) material demonstrated slightly lower mechanical performance, followed by the Sidi Ameur (Mat C) material. Lastly, the Oued Meitar (Mat A) composite displayed the least favorable mechanical properties among the tested materials.

Additionally, optical and chemical analysis provided insights into the homogeneity and composition of the materials. Furthermore, water absorption tests highlighted the importance of sand particle size and porosity in determining the material's suitability for various environmental conditions. Microscopic examination of fracture surfaces revealed crucial insights into the structural integrity of the composites, with observed defects impacting mechanical properties and water absorption rates. These findings emphasize the importance of optimizing material formulation and processing parameters to enhance overall performance.

Reference

[1] O. Drzyzga, A. Prieto, Plastic waste management, a matter for the ‘community’, Microbial biotechnology, 12 (2019) 66.

[2] E. El-Seidy, M. Chougan, M. Sambucci, M.J. Al-Kheetan, I. Biblioteca, M. Valente, S.H. Ghaffar, Lightweight alkali-activated materials and ordinary Portland cement composites using recycled polyvinyl chloride and waste glass aggregates to fully replace natural sand, Construction and Building Materials, 368 (2023) 130399.

[3] M. Sambucci, M. Valente, Ground waste tire rubber as a total replacement of natural aggregates in concrete mixes: Application for lightweight paving blocks, Materials, 14 (2021) 7493.

[4] J. Siddiqui, G. Pandey, A review of plastic waste management strategies, Int. Res. J. Environ. Sci, 2 (2013) 84.

[5] X. Liu, T. Lei, A. Boré, Z. Lou, B. Abdouraman, W. Ma, Evolution of global plastic waste trade flows from 2000 to 2020 and its predicted trade sinks in 2030, Journal of Cleaner Production, 376 (2022) 134373.

[6] J. Jiang, K. Shi, X. Zhang, K. Yu, H. Zhang, J. He, Y. Ju, J. Liu, From plastic waste to wealth using chemical recycling: A review, Journal of Environmental Chemical Engineering, 10 (2022) 106867.

[7] O. Kehinde, O. Ramonu, K. Babaremu, L. Justin, Plastic wastes: environmental hazard and instrument for wealth creation in Nigeria, Heliyon, 6 (2020) e05131.

[8] A.K.-L. Jnr, D. Yunana, P. Kamsouloum, M. Webster, D.C. Wilson, C. Cheeseman, Recycling waste plastics in developing countries: Use of low-density polyethylene water sachets to form plastic bonded sand blocks, Waste Management, 80 (2018) 112-118.

[9] I. Adam, T.R. Walker, J.C. Bezerra, A. Clayton, Policies to reduce single-use plastic marine pollution in West Africa, Marine Policy, 116 (2020) 103928.

[10] M. Thiam, M. Fall, M. Diarra, Mechanical properties of a mortar with melted plastic waste as the only binder: Influence of material composition and curing regime, and application in Bamako, Case Studies in Construction Materials, 15 (2021) e00634.

[11] L. Rigamonti, M. Grosso, J. Møller, V.M. Sanchez, S. Magnani, T.H. Christensen, Environmental evaluation of plastic waste management scenarios, Resources, Conservation and Recycling, 85 (2014) 42-53.

[12] C.-F. Chow, W.-M.W. So, T.-Y. Cheung, S.-K.D. Yeung, Plastic waste problem and education for plastic waste management, Emerging practices in scholarship of learning and teaching in a digital era, (2017) 125-140.

[13] R. Arman, E. Sundari, Y. Darmayanti, R. Efendi, Experimental Study of Heat Transfer Using Water–Cooled Condensers to Increase Oil Production from Plastic Waste, in: Journal of Physics: Conference Series, IOP Publishing, 2021, pp. 012168.

[14] H.T. Mohan, L. Masson, S. Kolathayarline, K.A.K. Sharma, A.G. Krishnan, S. Thiviya, R. Mohan, Transforming urban waste into construction blocks for a sanitation infrastructure: A step towards addressing rural open defecation, in: 2017 IEEE Global Humanitarian Technology Conference (GHTC), IEEE, 2017, pp. 1-9.

[15] O.O. Ayeleru, S. Dlova, O.J. Akinribide, F. Ntuli, W.K. Kupolati, P.F. Marina, A. Blencowe, P.A. Olubambi, Challenges of plastic waste generation and management in sub-Saharan Africa: A review, Waste Management, 110 (2020) 24-42.

[16] A. Soni, P.K. Das, M. Yusuf, S. Ridha, H. Kamyab, S. Chelliapan, I. Kirpichnikova, Z.H. Mussa, Valorization of Post-Consumers Plastics and Agro-Waste in Sustainable Polymeric Composites for Tribological Applications, Waste and Biomass Valorization, (2023) 1-17.

[17] E. Franco-Urquiza, H. Ferrando, D. Luis, M.L. Maspoch, Reciclado mecánico de residuos plásticos. Caso práctico: Poliestireno de alto impacto para la fabricación de componentes de TV, Afinidad, 73 (2016).

[18] T.M. Letcher, Plastic waste and recycling: Environmental impact, societal issues, prevention, and solutions, Academic Press, 2020.

[19] P. Lamba, D.P. Kaur, S. Raj, J. Sorout, Recycling/reuse of plastic waste as construction material for sustainable development: a review, Environmental Science and Pollution Research, (2021) 1-24.

[20] I. Mashudi, N. Suardana, I.A. Thanaya, I.B. Adnyana, C. Kencanawati, Compressive strength and truck run over ability of plastic/sand paving block composites, in: IOP Conference Series: Materials Science and Engineering, IOP Publishing, 2020, pp. 012011.

[21] S.K. Tulashie, E.K. Boadu, F. Kotoka, D. Mensah, Plastic wastes to pavement blocks: A significant alternative way to reducing plastic wastes generation and accumulation in Ghana, Construction and Building Materials, 241 (2020) 118044.

[22] G.N. Patil, M. Al Yahmedi, S.M. Walke, L. Rao, Manufacturing of plastic sand bricks from polypropylene and polyethylene waste plastic, Int J Adv Sci Tech, 29 (2020) 206-2068.

[23] S.M. Shitote, Z.C.A. Gariy, E. Ronoh, Influence of Coarse Aggregate on the Physical and Mechanical Performance of Paving Blocks made using Waste Plastic.

[24] K. Sahani, B.R. Joshi, K. Khatri, A.T. Magar, S. Chapagain, N. Karmacharya, Mechanical Properties of Plastic Sand Brick Containing Plastic Waste, Advances in Civil Engineering, 2022 (2022).

[25] H.T. Mohan, F. Whitaker, R. Mohan, K. Mini, Performance assessment of recycled LDPE with sand fillers, Materials Today: Proceedings, 42 (2021) 1526-1530.

[26] M. Seghiri, D. Boutoutaou, A. Kriker, M.I. Hachani, The possibility of making a composite material from waste plastic, Energy Procedia, 119 (2017) 163-169.

[27] H.A. Bulut, R. Şahin, A study on mechanical properties of polymer concrete containing electronic plastic waste, Composite Structures, 178 (2017) 50-62.

[28] A. Diana, D. Deshariyanto, Effect of addition waste bottle and fly ash variation to compressive strength environmentally friendly paving block, in: Journal of Physics: Conference Series, IOP Publishing, 2020, pp. 012025.

[29] M. Hsie, C. Tu, P. Song, Mechanical properties of polypropylene hybrid fiber-reinforced concrete, Materials Science and Engineering: A, 494 (2008) 153-157.

[30] M. Guendouz, F. Debieb, O. Boukendakdji, E. Kadri, M. Bentchikou, H. Soualhi, Use of plastic waste in sand concrete, J. Mater. Environ. Sci, 7 (2016) 382-389.

[31] J. Nisar, M. Aziz, A. Shah, I. Shah, M. Iqbal, Conversion of polypropylene waste into value-added products: a greener approach, Molecules, 27 (2022) 3015.

[32] P. Tratzi, C. Giuliani, M. Torre, L. Tomassetti, R. Petrucci, A. Iannoni, L. Torre, S. Genova, V. Paolini, F. Petracchini, Effect of hard plastic waste on the quality of recycled polypropylene blends, Recycling, 6 (2021) 58.

[33] H. Otuoze, A. Shuaibu, An experimental study on the use of polypropylene waste in bituminous mix, Nigerian Journal of Technology, 36 (2017) 677-685.

[34] A. Aravind, A.R. Bhagat, R. Radhakrishnan, A novel use of twisted continuous carbon fibers in additive manufacturing of composites, Materials Today: Proceedings, 46 (2021) 7049-7055.

[35] A. Kumi-Larbi Jnr, R. Galpin, S. Manjula, Z. Lenkiewicz, C. Cheeseman, Reuse of Waste Plastics in Developing Countries: Properties of Waste Plastic-Sand Composites, Waste and Biomass Valorization, (2022) 1-14.

[36] S. Gahane, S. Gour, K. Raut, D. Kumari, S. Gaidhane, A. Moon, PLASTIC WASTE UTILIZATION IN PAVER BLOCK.

[37] F.I. Aneke, C. Shabangu, Green-efficient masonry bricks produced from scrap plastic waste and foundry sand, Case Studies in Construction Materials, 14 (2021) e00515.

[38] D. Jain, S. Bhadauria, S. Kushwah, An experimental study of utilization of plastic waste for manufacturing of composite construction material, International Journal of Environmental Science and Technology, (2022) 1-10.

[39] S.N. Ahmed, N.H. Sor, M.A. Ahmed, S.M. Qaidi, Thermal conductivity and hardened behavior of eco-friendly concrete incorporating waste polypropylene as fine aggregate, Materials Today: Proceedings, 57 (2022) 818-823.

[40] C. Budiyantoro, H. Sosiati, J.W. Joharwan, The influence of the number of recycling cycles on the thermal and physical properties of polypropylene, Jurnal Polimesin, 21 (2023) 438-444.

[41] L. Benhamadouche, M. Rokbi, H. Osmani, M. Jawaid, M. Asim, A.B.M. Supian, S. Mekideche, N. Moussaoui, H. Fouad, R. Khiari, Characterization of physical and mechanical properties of recycled jute fabric reinforced polypropylene composites, Polymer Composites, 42 (2021) 5435-5444.

[42] N. Meftah, M.S. Mahboub, Spectroscopic characterizations of sand dunes minerals of El-Oued (Northeast Algerian Sahara) by FTIR, XRF and XRD analyses, Silicon, 12 (2020) 147-153.

[43] T.D.T. Oyedotun, X-ray fluorescence (XRF) in the investigation of the composition of earth materials: a review and an overview, Geology, Ecology, and Landscapes, 2 (2018) 148-154.

[44] H. Kowanou, E. Sanya, A. Vianou, Effets de l'incorporation du fondu de déchets de sachets plastiques sur la consistance du bitume et la stabilité du béton bitumineux, Afrique Science: Revue Internationale des Sciences et Technologie, 10 (2014).

[45] L.A. Sanchez-Echeverri, N.J. Tovar-Perilla, J.G. Suarez-Puentes, J.E. Bravo-Cervera, D.F. Rojas-Parra, Mechanical and market study for sand/recycled-plastic cobbles in a medium-size Colombian city, Recycling, 6 (2021) 17.

[46] Y.O. Babatunde, R.A. Ibrahim, D.O. Oguntayo, Effect of mix proportion on the strength and durability of plastic and sand composite for construction applications, Innovative Infrastructure Solutions, 7 (2022) 333.

[47] A. Soni, P.K. Das, Development of sand-plastic composites as floor tiles using silica sand and recycled thermoplastics mixture from post-consumer products-A sustainable approach for cleaner production, (2022).

[48] S.A. Boussaa, A. Kheloufi, N.B. Zaourar, Sand dune characterization for preparing metallurgical grade silicon, Open Chemistry, 16 (2018) 1227-1232.

[49] E. Ahmed, M. Soliman, A. Alsharhan, S. Tamer, Mineralogical characteristics of the Quaternary sand dunes in the eastern province of Abu Dhabi, United Arab Emirates, in: Quaternary Deserts and Climatic Change, CRC Press, 2020, pp. 85-90.

[50] A.-C. Pescheux, E. Le Baron, O. Raccurt, Characterization of different Moroccan sands to explain their potential negative impacts on CSP solar mirrors, Solar Energy, 194 (2019) 959-968.

[51] M.L. Mechri, S. Chihi, N. Mahdadi, S. Beddiaf, Study of heat effect on the composition of dunes sand of Ouargla (Algeria) using XRD and FTIR, Silicon, 9 (2017) 933-941.

[52] S. Lucas, M.T. Tognonvi, J. Gelet, J. Soro, S. Rossignol, Interactions between silica sand and sodium silicate solution during consolidation process, Journal of non-crystalline solids, 357 (2011) 1310-1318.

[53] M.M. Khan, M. Singh, G. Jadhav, S. Mahajani, S. Mandre, Characterization of waste and reclaimed green sand used in foundry processing, Silicon, 12 (2020) 677-691.

[54] N. Mahdadi, Y. Benkrima, S. Chihi, M.L. Mechri, M.S.E. Bougoffa, Spectroscopic properties of Ouargla Sand Dunes—Algeria, Arabian Journal of Geosciences, 15 (2022) 1288.

[55] R. Morent, N. De Geyter, C. Leys, L. Gengembre, E. Payen, Comparison between XPS-and FTIR-analysis of plasma-treated polypropylene film surfaces, Surface and Interface Analysis: An International Journal devoted to the development and application of techniques for the analysis of surfaces, interfaces and thin films, 40 (2008) 597-600.

[56] M. Tiwari, T. Rathod, P. Ajmal, R. Bhangare, S. Sahu, Distribution and characterization of microplastics in beach sand from three different Indian coastal environments, Marine pollution bulletin, 140 (2019) 262-273.

[57] J. Jose, S. Satapathy, A. Nag, G. Nando, Modification of waste polypropylene with waste rubber dust from textile cot industry and its characterization, Process Safety and Environmental Protection, 85 (2007) 318-326.

[58] A. Kassouf, J. Maalouly, D.N. Rutledge, H. Chebib, V. Ducruet, Rapid discrimination of plastic packaging materials using MIR spectroscopy coupled with independent components analysis (ICA), Waste management, 34 (2014) 2131-2138.

[59] Z. Yao, T. Chen, H. Li, M. Xia, Y. Ye, H. Zheng, Mechanical and thermal properties of polypropylene (PP) composites filled with modified shell waste, Journal of hazardous materials, 262 (2013) 212-217.

[60] J.A. Hadi, F.G. Najmuldeen, I. Ahmed, Quality restoration of waste polyolefin plastic material through the dissolution-reprecipitation technique, Chemical Industry and Chemical Engineering Quarterly, 20 (2014) 163-170.

[61] A.F. Hamzah, R.M. Alkhafaj, An investigation of manufacturing technique and characterization of low-density polyethylene waste base bricks, Materials Today: Proceedings, 61 (2022) 724-733.

[62] D.X. Thang, FABRICATION AND STUDY ON PROPERTIES OF POLYPROPYLENE COMPOSITE MATERIALS/SILICA SAND POWDER, (2023).

[63] P. Vilímová, J. Tokarský, P. Peikertová, K.M. Kutláková, T. Plaček, Influence of thermal and UV treatment on the polypropylene/graphite composite, Polymer Testing, 52 (2016) 46-53.

[64] D. Aydemir, U. Gulsen, H. GUMUŞ, S. Yildiz, S. GUMUŞ, T. Bardak, G. Gunduz, Nanocomposites of polypropylene/nano titanium dioxide: effect of loading rates of nano titanium dioxide, Materials Science, 22 (2016) 364-369.

[65] A. Soni, P.K. Das, M. Yusuf, A.A. Pasha, K. Irshad, M. Bourchak, Synergy of RHA and silica sand on physico-mechanical and tribological properties of waste plastic–reinforced thermoplastic composites as floor tiles, Environmental Science and Pollution Research, (2022) 1-19.

[66] N. Garcia-Troncoso, L. Li, Q. Cheng, K.H. Mo, T.-C. Ling, Comparative study on the properties and high temperature resistance of self-compacting concrete with various types of recycled aggregates, Case Studies in Construction Materials, 15 (2021) e00678.

[67] M.A. Dalhat, H.A.-A. Wahhab, Cement-less and asphalt-less concrete bounded by recycled plastic, Construction and Building Materials, 119 (2016) 206-214.

[68] K.E. BARIŞ, L. TANAÇAN, Natural pozzolan-based green geopolymer foam for thermal insulation, Journal of Sustainable Construction Materials and Technologies, 7 128-144.

[69] L.D. Wakeley, G.S. Wong, J. Burkes, Petrographic techniques applied to cement-solidified hazardous waste, (1992).

Declaration of interests

☒ The authors declare that they have no known competing financial interests or personal relationships that could have appeared to influence the work reported in this paper.

☐The authors declare the following financial interests/personal relationships which may be considered as potential competing interests: